DOI: 10.1002/ejic.200601131

Hydrothermal Synthesis of Single Crystalline (K,Na)NbO_3 Powders

Ce Sun,[a] Xianran Xing,*[a,b] Jun Chen,[a] Jinxia Deng,[a] Lu Li,[a] Ranbo Yu,[a] Lijie Qiao,[c] and Guirong Liu[a]

Keywords: Hydrothermal synthesis / Crystal growth / Crystal morphology / Niobates

$(K_{1-x}Na_x)NbO_3$ (x = 0.01, 0.24, 0.89, 0.91, 0.99) single crystalline powders with perovskite structure were synthesized by a hydrothermal method with Nb_2O_5 in a mixed solution of KOH and NaOH at 220 °C for 24 h. XRD investigations showed that the structure of the synthesized $(K_{1-x}Na_x)NbO_3$ ceramics changed from a $KNbO_3$-type orthorhombic phase (space group *Bmm*2) to a $NaNbO_3$-type monoclinic phase (space group *Pm*) with the increase of Na content. The present results confirmed that $(K_{1-x}Na_x)NbO_3$ exhibited a morphotropic phase boundary (MPB) at around 50 %K separating the orthorhombic phase and monoclinic phase. FE-SEM images showed that the morphological structures of niobates were cubes and nanofingers. The TEM image and the selected area electron diffraction pattern of $(K_{0.01}Na_{0.99})NbO_3$ showed the as-synthesized powder was single crystalline and indexed to be monoclinic. The phase evolution of the products in the hydrothermal route revealed that the hydrothermal synthesis of $(K_{1-x}Na_x)NbO_3$ underwent two steps, where an intermediate product $(K_{8-8x}Na_{8x})Nb_6O_{19}{\cdot}nH_2O$ was found in the early stage and then pure $(K_{1-x}Na_x)NbO_3$ was obtained after another 30 min of hydrothermal treatment.

(© Wiley-VCH Verlag GmbH & Co. KGaA, 69451 Weinheim, Germany, 2007)

Introduction

Alkaline niobates have captured considerable interest in the scientific community because of their excellent ferroelectric, piezoelectric, electromechanical, nonlinear optical, electricoptic, and ionic conductivity properties.[1–6] The alkaline niobate-based perovskite compounds without toxic elements show a high Curie temperature and low anisotropy. Among them, $(K_{0.5}Na_{0.5})NbO_3$ was considered a good candidate for lead-free piezoelectric ceramics because of its strong piezoelectricity and ferroelectricity.[2,7,8] $(K_{1-x}Na_x)NbO_3$ is a combination of ferroelectrics $KNbO_3$ and antiferroelectrics $NaNbO_3$, and forms a morphotropic phase boundary (MPB) at around 50%K separating two orthorhombic phases[7,9] or orthorhombic and tetragonal phases with the composition modification of Li and Sb.[10] The piezoelectric properties of $(K_{1-x}Na_x)NbO_3$ single crystals were first reported by Egerton et al.[7] and Cross.[11] The hot pressed $(K_{0.5}Na_{0.5})NbO_3$ ceramics have been reported to possess high phase transition temperature ($T_c \approx$ 420 °C), high remanent polarization ($P_r \approx 33\ \mu C/cm^2$), large piezoelectric longitudinal response ($d_{33} \approx 160$ pC/N), and planar coupling coefficients ($k_p \approx 45\%$).[12,13]

To date, several studies have been devoted to the fabricating processes and properties of $(K_{1-x}Na_x)NbO_3$. $(K_{1-x}Na_x)NbO_3$ powders are commonly synthesized by a solid-state method. Saito et al.[2] reported that a high d_{33} (about 416 pC/N) constant was obtained in the textured $(K_{1-x}Na_x)NbO_3$-based ceramics close to a morphotropic phase boundary. Pithan et al.[14] and Zhang et al.[15] prepared $(K_{1-x}Na_x)NbO_3$ by microemulsion mediated and spark plasma sintering methods, respectively. Shiratori et al.[16] synthesized the monoclinic $(K_{0.5}Na_{0.5})NbO_3$ by a microemulsion mediated route. The hydrothermal synthesis method has been used to prepare perovskite-type $NaNbO_3$, $KNbO_3$, KNb_3O_8, and $K_4Nb_6O_{17}$ powders over the past decade.[1,17–20] However, synthesis of the complex of $(K_{1-x}Na_x)NbO_3$ has not involved a hydrothermal route.

In the present study, we synthesized single crystalline powders of $(K_{1-x}Na_x)NbO_3$ by a hydrothermal method under moderate conditions. The structural evolution during the reaction between Nb_2O_5 and concentrated aqueous NaOH and KOH mixed solution was investigated. The crystal structures of the obtained powders were identified by XRD. The morphology of the samples was studied by field-emission scanning electron microscopy (FE-SEM) and TEM, and elemental analyses for Nb, K, and Na were conducted by inductively coupled plasma (ICP) spectrometry.

[a] Department of Physical Chemistry, University of Science and Technology Beijing,
Beijing 100083, China
Fax: +86-10-6233-3477
E-mail: xing@ustb.edu.cn
[b] State Key Laboratory for Advanced Metals and Materials, University of Science and Technology Beijing,
Beijing 100083, China
[c] Key Laboratory of Environmental Fracture, Ministry of Education of China,
Beijing 100083, China

 InterScience © 2007 Wiley-VCH Verlag GmbH & Co. KGaA, Weinheim

Results and Discussion

The influence of the processing parameters of K/Na molar ratio in the aqueous mixed solution on the formation of $(K_{1-x}Na_x)NbO_3$ is summarized in Table 1. The elemental analysis for Na, K, and Nb was conducted by ICP spectrometry. Because the values of Na and Nb were more accurate than that of K, the stoichiometries of all products were calculated based on the measurements of Na and Nb. KOH/NaOH plays the role of K^+/Na^+ source and the alkalinity in the aqueous medium, which affects the nucleation and crystallization of the products. The K/Na molar ratio in the as-synthesized samples increased with the ratio in the mixed solution. However, there was a big jump from KNN2 (Na/K = 24:76) to KNN3 (Na/K = 89:11). This might be attributed to the larger ionic radii of K^+ compared to that of Na^+, leading to a sharp rise of the reaction activity of Na^+ in the solution.

Table 1. K/Na/Nb ratio and the possible formula of the sodium-potassium niobates.

Sample No.	Concentration [mol/L] KOH	NaOH	K/Na/Nb ratio[a]	Formula
KNN1	9.0	1.0	96.2:1.3:100	$K_{0.99}Na_{0.01}NbO_3$
KNN2	8.0	2.0	76.9:24.4:100	$K_{0.76}Na_{0.24}NbO_3$
KNN3	7.0	3.0	7.6:88.7:100	$K_{0.11}Na_{0.89}NbO_3$
KNN4	6.0	4.0	7.8:91.3:100	$K_{0.09}Na_{0.91}NbO_3$
KNN5	5.0	5.0	3.5:99.4:100	$K_{0.01}Na_{0.99}NbO_3$

[a] Measured by ICP.

The XRD patterns (Figure 1) showed that pure phase $(K_{1-x}Na_x)NbO_3$ powders were obtained in the 10 mol/L KOH and NaOH solution. This indicated that well-crystallized $(K_{1-x}Na_x)NbO_3$ powders were synthesized in the concentrated alkaline solution under mild conditions. $(K_{0.99}Na_{0.01})NbO_3$ and $(K_{0.76}Na_{0.24})NbO_3$ were indexed in orthorhombic symmetry (space group *Bmm*2), but $(K_{0.11}Na_{0.89})NbO_3$, $(K_{0.09}Na_{0.91})NbO_3$, and $(K_{0.01}Na_{0.99})NbO_3$ were indexed in monoclinic symmetry (space group *Pm*), the lattice parameters are labeled in Table 2. The increasing of Na content in (K,Na)NbO_3 resulted in the phase transition from a $KNbO_3$-type orthorhombic phase to a $NaNbO_3$-type monoclinic phase.[21] This further confirmed a morphotropic phase boundary at around 50%K separating orthorhombic and monoclinic phases, but not two orthorhombic phases[7,9] or orthorhombic and tetragonal phases with composition modification of Li and Sb[10] as reported before.

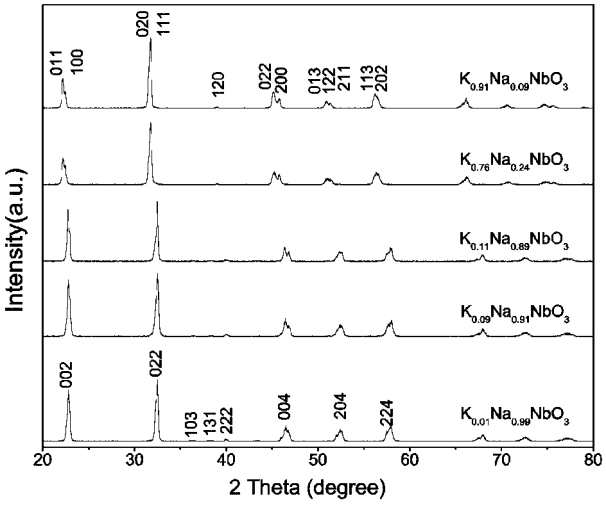

Figure 1. The XRD patterns of $(K_{1-x}Na_x)NbO_3$ prepared at 220 °C for 24 h.

Table 2. The crystal system and lattice parameters of the alkaline niobates.

Sample	Syngony	Lattice parameters[a] *a* [Å]	*b* [Å]	*c* [Å]	*β* [°]
$K_{0.99}Na_{0.01}NbO_3$	orthorhombic	3.976(9)	5.686(0)	5.698(0)	–
$K_{0.76}Na_{0.24}NbO_3$	orthorhombic	3.970(6)	5.675(5)	5.687(1)	–
$K_{0.11}Na_{0.89}NbO_3$	monoclinic	7.773(8)	7.838(2)	7.849(8)	89.901
$K_{0.09}Na_{0.91}NbO_3$	monoclinic	7.781(0)	7.825(6)	7.867(6)	89.624
$K_{0.01}Na_{0.99}NbO_3$	monoclinic	7.789(3)	7.819(9)	7.866(3)	89.717

[a] Lattice parameters were calculated by Powder X and TREOR software.

FE-SEM images of $(K_{0.99}Na_{0.01})NbO_3$ prepared by the hydrothermal treatment (220 °C, 24 h) are shown in Figure 2. Large-scale and well-crystallized $(K_{0.99}Na_{0.01})NbO_3$ cubes in microns were obtained (Figure 2, a), and a few nanofingers were also observed (Figure 2, b), which was confirmed by the previous work.[22] The aspect ratios (approximately length-to-width ratio) of the nanofingers are as high as 10 and their average width is about 60–75 nm.

The TEM images and the selected area electron diffraction (SAED) patterns of $(K_{0.01}Na_{0.99})NbO_3$ are displayed in Figure 3. The TEM image (see Figure 3, a) showed a club-shaped morphology for the $(K_{0.01}Na_{0.99})NbO_3$ single crystal. The SAED pattern (see Figure 3, b) revealed that $(K_{0.01}Na_{0.99})NbO_3$ was single crystalline and was indexed as monoclinic in structure, which was consistent with the present XRD investigation.

The phase evolution of $(K_{0.76}Na_{0.24})NbO_3$ (KNN2) via a hydrothermal synthesizing processing route was studied by XRD (see Figure 4). A series of XRD patterns of KNN2 were obtained at 220 °C and labeled KNN2-*n*, where *n* denoted the hydrothermal treatment time (in min). The raw material of Nb_2O_5 was mostly α-Nb_2O_5 with a few β-Nb_2O_5 as shown in Figure 4 (a). During the first 60 min Nb_2O_5 gradually reacted with the alkaline solution, and a new phase emerged as shown in Figure 4 (b,c). The XRD peaks of the new phase were isolated as $K_4Na_4Nb_6O_{19}{\cdot}9H_2O$.[23] However, the molar concentrations of K^+ and Na^+ were not equal in the final product KNN2 (see ICP result in Table 1), which suggested that the new phase would be $(K_{8-8x}Na_{8x})Nb_6O_{19}{\cdot}nH_2O$ but not $K_4Na_4Nb_6O_{19}{\cdot}9H_2O$. The dominant phases in KNN2–*90* were $(K_{8-8x}Na_{8x})Nb_6O_{19}{\cdot}nH_2O$ and $(K_{1-x}Na_x)NbO_3$ with minor Nb_2O_5 as shown in Figure 4 (d). After 120 min only one phase of KNN2 was observed (see Figure 4, e). This implied that the

 © 2007 Wiley-VCH Verlag GmbH & Co. KGaA, Weinheim

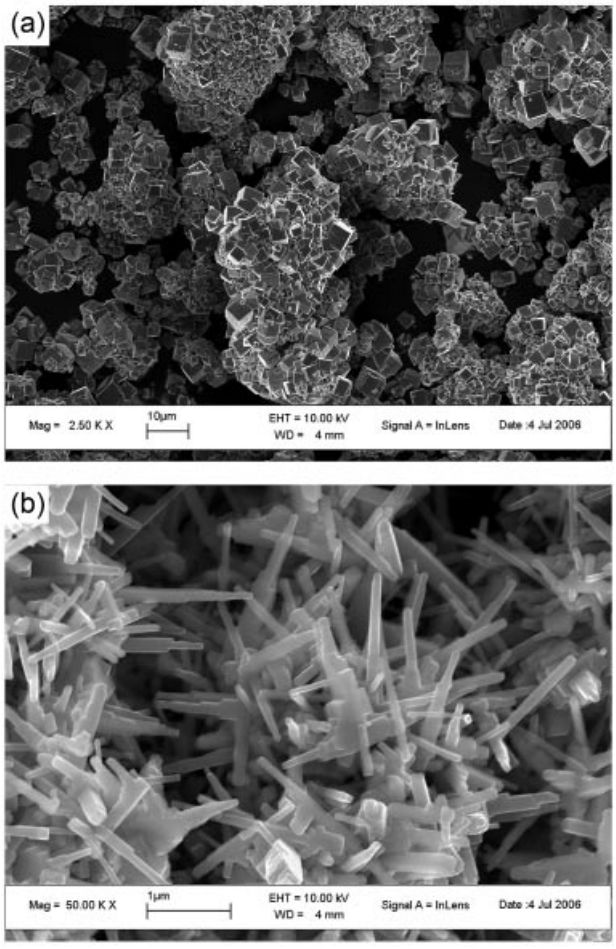

Figure 2. FE-SEM images of $(K_{0.99}Na_{0.01})NbO_3$ synthesized at 220 °C for 24 h: (a) cubes, (b) nanofingers.

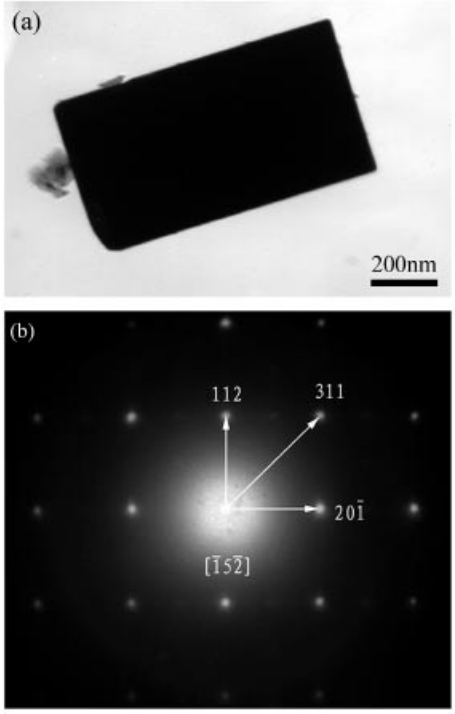

Figure 3. TEM images (a) and selected area electron diffraction (b) of the $(K_{0.01}Na_{0.99})NbO_3$ sample.

intermediate phase $(K_{8-8x}Na_{8x})Nb_6O_{19}{\cdot}nH_2O$ further reacted with Nb_2O_5 to form KNN2 powders. The KNN2–*150* sample was a well-crystallized phase of KNN2 (see part f in Figure 4). The same phase evolution was also observed for $(K_{0.09}Na_{0.91})NbO_3$ (KNN4) as shown in Figure 5, the intermediate product $(K_{8-8x}Na_{8x})Nb_6O_{19}{\cdot}nH_2O$ was found in the early stage and then pure $(K_{0.09}Na_{0.91})NbO_3$ was obtained after further hydrothermal treatment (see parts d,e in Figure 5).

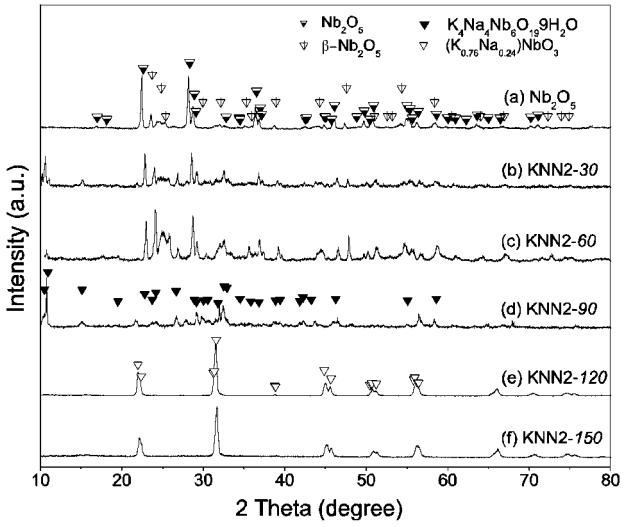

Figure 4. The XRD patterns of $(K_{0.76}Na_{0.24})NbO_3$ (KNN2) samples after various reaction periods (which were indicated in the figure) at 220 °C.

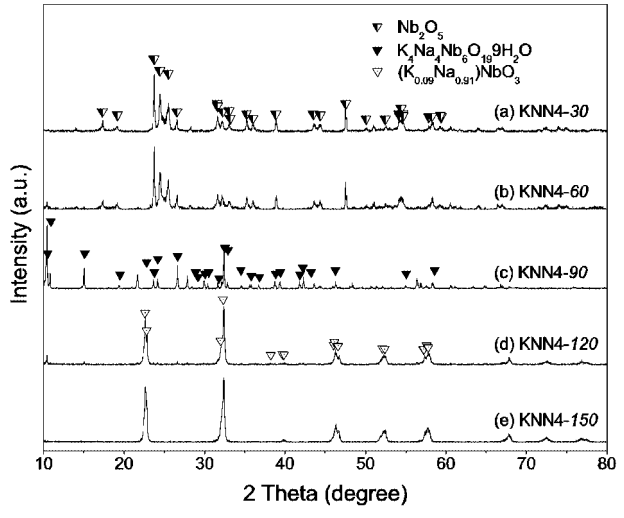

Figure 5. The XRD patterns of $(K_{0.09}Na_{0.91})NbO_3$ (KNN4) samples after various reaction periods (which were indicated in the figure) at 220 °C.

Hence, it was concluded that the formation of $(K_{1-x}Na_x)NbO_3$ occurred in two steps. The first step was that Nb_2O_5 reacted with MOH (M = Na, K) to form $(K_{8-8x}Na_{8x})Nb_6O_{19}{\cdot}nH_2O$ [Equation (1)].

 © 2007 Wiley-VCH Verlag GmbH & Co. KGaA, Weinheim

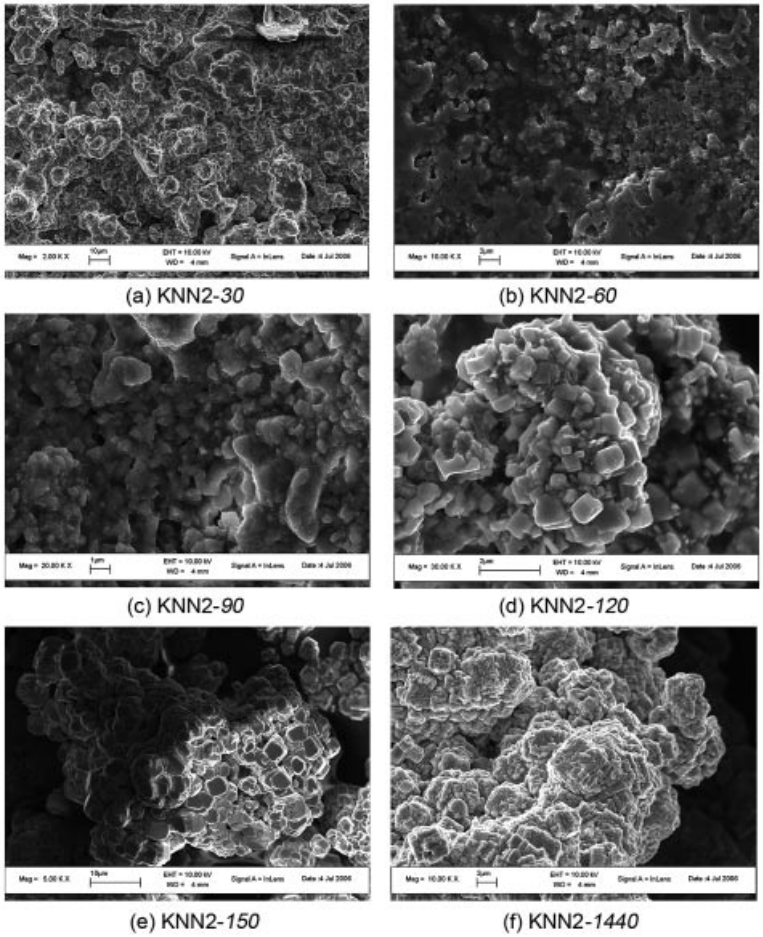

Figure 6. The morphological evolution of the $(K_{0.76}Na_{0.24})NbO_3$ (KNN2) samples during the reaction course by FE-SEM images: (a) KNN2–*30*, (b) KNN2–*60*, (c) KNN2–*90*, (d) KNN2–*120*, (e) KNN2–*150*, (f) KNN2–*1440*.

$$(8-8x)\ KOH + 8x\ NaOH + 3\ Nb_2O_5 + (n-4)\,H_2O = (K_{8-8x}Na_{8x})Nb_6O_{19}{\cdot}n\,H_2O \quad (1)$$

The second step was that $(K_{8-8x}Na_{8x})Nb_6O_{19}{\cdot}n\,H_2O$ reacted with Nb_2O_5 [Equation (2)].

$$(K_{8-8x}Na_{8x})Nb_6O_{19}{\cdot}n\,H_2O + Nb_2O_5 = 8\ (K_{1-x}Na_x)NbO_3 + n\,H_2O \quad (2)$$

The morphological evolution of $(K_{0.76}Na_{0.24})NbO_3$ was investigated by FE-SEM (see Figure 6). The reactants nearly kept the morphology of Nb_2O_5 in the first 30 min as shown in Figure 6 (a). But Nb_2O_5 gradually fluxed and reacted with the alkaline solution as shown in Figure 6 (b,c). After 120 min a small-scale cubic phase was formed. The KNN2–*150* sample was very pure potassium sodium niobate with a club-shaped morphology as shown in Figure 6 (e). The FE-SEM image and XRD pattern of KNN2–*1440* (KNN2 in Table 1) were similar to KNN2–*150*, and the XRD and ICP investigations demonstrated that it was $(K_{0.76}Na_{0.24})NbO_3$ crystal powder.

Conclusions

$(K_{1-x}Na_x)NbO_3$ (x = 0.01, 0.24, 0.89, 0.91, 0.99) single crystalline powders with perovskite structure were synthesized by a hydrothermal method with Nb_2O_5 in a mixed solution of KOH and NaOH at 220 °C for 24 h. The as-synthesized $(K_{1-x}Na_x)NbO_3$ powders showed that with the increase of Na content the crystal structure changed from a $KNbO_3$-type orthorhombic phase (space group *Bmm*2) to a $NaNbO_3$-type monoclinic phase (space group *Pm*). It further confirmed that $(K_{1-x}Na_x)NbO_3$ exhibited a morphotropic phase boundary at around 50%K separating the orthorhombic and monoclinic phases. The morphological structures of the niobates were cubes and nanofingers. The SAED pattern showed that $(K_{0.01}Na_{0.99})NbO_3$ was single crystalline and indexed as monoclinic in structure, which was consistent with the XRD investigation. We concluded that the hydrothermal synthesis of $(K_{1-x}Na_x)NbO_3$ underwent two steps, and had an intermediate phase as $(K_{8-8x}Na_{8x})Nb_6O_{19}{\cdot}n\,H_2O$. The first step was that Nb_2O_5 reacted with MOH (M = Na, K) to form $(K_{8-8x}Na_{8x})$-$Nb_6O_{19}{\cdot}n\,H_2O$. The second step was where $(K_{8-8x}Na_{8x})$-$Nb_6O_{19}{\cdot}n\,H_2O$ reacted with Nb_2O_5, and finally formed $(K_{1-x}Na_x)NbO_3$ single crystal powders.

Experimental Section

Synthetic Procedures: KOH, NaOH, and Nb_2O_5 (all are analytic reagent grade) were used in the synthesis. In a typical synthesis

 © 2007 Wiley-VCH Verlag GmbH & Co. KGaA, Weinheim

process, Nb_2O_5 (0.5 g) was added to a mixed solution of NaOH and KOH (30 mL), and stirred for half an hour. Then the white slurry was introduced into a Teflon-lined stainless steel autoclave and heated in a furnace at 220 °C for 24 h. After gradually cooling down to room temperature, the precipitates were filtered and washed with distilled water and ethanol, then dried at 80 °C.

Measurements: The morphologies of the samples were studied by field-emission scanning electron microscopy (FE-SEM, LEO1530) and transmission electron microscopy (TEM, JEM-100CXII). Elemental analysis for Nb, K, and Na was conducted by inductively coupled plasma (ICP, INC Profile) spectrometry.

X-ray Structure: The crystal structures of the obtained powders were identified by powder X-ray diffractometry, performed with a M21XVHF22 diffractometer (Japan) at room temperature. Cu-K_α radiation (λ = 1.5418 Å) and a fixed power source (40 kV and 200 mA) were used. The samples were scanned at a rate of 8°/min over a range of 10–90°. The major diffraction peaks of the samples were indexed by Powder X and TREOR software.

Acknowledgments

This work was financially supported by the National Natural Science Foundation of China (No. 50374009, 20571009, 20331030), and Funds of Ministry of Education of China for PCSIRT.

[1] H. Zhu, Z. Zheng, X. Gao, Y. Huang, Z. Yan, J. Zou, H. Yin, Q. Zou, S. H. Kable, J. Zhao, Y. Xi, W. N. Martens, R. L. Frost, *J. Am. Chem. Soc.* **2006**, *128*, 2373–2384.
[2] Y. Saito, H. Takao, T. Tani, T. Nonoyama, K. Takatori, T. Homma, T. Nagaya, M. Nakamura, *Nature* **2004**, *432*, 84–87.
[3] C. An, K. Tang, C. Wang, G. Shen, Y. Jin, Y. Qian, *Mater. Res. Bull.* **2002**, *37*, 1791–1796.
[4] G. Suyal, E. Colla, R. Gysel, M. Cantoni, N. Setter, *Nano Lett.* **2004**, *4*, 1339–1342.
[5] C.-R. Cho, I. Katardjiev, M. Grishin, A. Grishin, *Appl. Phys. Lett.* **2002**, *80*, 3171.
[6] M. Blomqvist, S. Khartsev, A. Grishin, A. Petraru, C. Buchal, *Appl. Phys. Lett.* **2003**, *82*, 439.
[7] L. Egerton, D. M. Dillon, *J. Am. Ceram. Soc.* **1959**, *42*, 438–442.
[8] E. Hollenstein, M. Davis, D. Damjanovic, N. Setter, *Appl. Phys. Lett.* **2005**, *87*, 182905.
[9] K. Kakimoto, I. Masuda, H. Ohsato, *Jpn. J. Appl. Phys. Part 1* **2003**, *42*, 6102–6105.
[10] G.-Z. Zang, J.-F. Wang, H.-C. Chen, W.-B. Su, C.-M. Wang, P. Qi, B.-Q. Ming, J. Du, L.-M. Zheng, S. Zhang, T. R. Shrout, *Appl. Phys. Lett.* **2006**, *88*, 212908.
[11] L. E. Cross, *Nature* **1958**, *181*, 178–179.
[12] R. E. Jeager, L. Egerton, *J. Am. Ceram. Soc.* **1962**, *45*, 208–213.
[13] G. H. Haertling, *J. Am. Ceram. Soc.* **1967**, *50*, 329–331.
[14] C. Pithan, Y. Shiratori, J. Dornseiffer, F.-H. Haegel, A. Magrez, R. Waser, *J. Cryst. Growth* **2005**, *280*, 191–200.
[15] B.-P. Zhang, J.-F. Li, K. Wang, H. Zhang, *J. Am. Ceram. Soc.* **2006**, *89*, 1605–1609.
[16] Y. Shiratori, A. Magrez, C. Pithan, *Chem. Phys. Lett.* **2004**, *391*, 288–292.
[17] J.-F. Liu, X.-L. Li, Y. D. Li, *J. Cryst. Growth* **2003**, *247*, 419–424.
[18] C. M. S. Santos, L. H. Loureiro, M. P. F. Silva, M. V. Cacaleiro, *Polyhedron* **2002**, *21*, 2009–2015.
[19] C.-H. Lu, S.-Y. Lo, H.-C. Lin, *Mater. Lett.* **1998**, *34*, 172–176.
[20] G. K. L. Goh, F. F. Lange, S. M. Haile, C. G. Levi, *J. Mater. Res.* **2003**, *18*, 338–345.
[21] a) A. W. Hewat, *J. Phys. C: Solid State Phys.* **1973**, *6*, 2559–2572; b) A. W. Hewat, *Ferroelectrics* **1974**, *7*, 83–85.
[22] E. Vasco, A. Magrez, L. Forró, N. Setter, *J. Phys. Chem. B* **2005**, *109*, 14331–14334.
[23] J. H. Kennedy, *J. Inorg. Nucl. Chem.* **1961**, *20*, 53–57.

Received: November 29, 2006
Published Online: March 20, 2007

 © 2007 Wiley-VCH Verlag GmbH & Co. KGaA, Weinheim